ANN Based Sensor and Actuator Fault Detection in Nuclear Reactors

[1]Shohan Banerjee, Jiamei Deng, and Chris Gorse
School of Built Environment, Engineering and Computing
Leeds Beckett University
Leeds, United Kingdom
e-mail: s.banerjee@leedsbeckett.ac.uk,
j.deng@leedsbeckett.ac.uk,
c.gorse@leedsbeckett.ac.uk

[2]Vineet Vajpayee and Victor Becerra
School of Energy and Electronic Engineering
University of Portsmouth
Portsmouth, United Kingdom
e-mail: vineet.vajpayee@port.ac.uk,
victor.becerra@port.ac.uk

[3]S. R. Shimjith
Reactor Control System Design Section
Bhabha Atomic Research Centre and
Homi Bhabha National Institute
Mumbai, India
e-mail: srshim@barc.gov.in

***Abstract*— In the nuclear power plants (NPPs), fault detection and diagnosis (FDD) methods are very important to improve the safety and reliability of plants. Researchers have established various FDD methods such as model-based methods, data-driven methods, and signal-based methods. In practical applications, model-based methods are very difficult to achieve. Thus, various data-driven methods and signal-based methods have been applied for monitoring key subsystems in NPPs. In this paper, a brief overview of the Artificial Neural Network (ANN) based FDD method is presented. Simulated data have been generated to train the ANNs as per requirement and to compare with the plant signal during a fault. A technique has been proposed analyzing two sensors data (power sensor and coolant sensor) to determine the sensor and actuator fault in a closed-loop in presence of robust (Proportional-Integral-Derivative) PID controller. Results are produced with credible MATLAB simulation.**

Keywords— ANN; Fault Detection; NPP; PWR

I. INTRODUCTION

A Nuclear Power Plant (NPP) is a highly complex process plant where many sensors and actuators are used to monitor and control different parameters, respectively. However, sensors and actuators endure various faults such as component failure and variations in operating conditions over time due to their inner structural modifications which leads to precision degradation of measurement and efficiency of plants. Therefore, reliable functioning of sensors and actuators is crucial for optimal process control. To maintain a high level of performance of NPPs, it is necessary to detect and diagnose faults promptly so that corrective action can be taken to accommodate the system alternation to prevent the certain shutdown or any big accidental scenario [1].

Over the past decades, researchers have devoted them to fault detection and isolation modelling. Many methods for faults detection and isolation have already been established. Model-based fault detection is extremely popular among those methods. Raphaela et al. in [2] proposed a fault detection method based on physical redundancy where the output is compared with that of the redundant sensor. Gautam et al. in [3] have shown a statistical algorithm for time-varying incipient fault detection and isolation of sensors. Extended Kalman filter has been used here to formulate the fault detection index and fault signature.

Another technique proposed by Zhao et al. in [4] is based on an integrated approach to detect and isolate the fault of the field devices like sensors, actuators, controllers in NPPs. With this procedure, nuclear plants are described as a causal graph where individual process variable is in connection with adaptive fuzzy inference system models. Support vector machine and improved particle swarm optimization (PSO) have been applied for hybrid fault diagnosis in [5]. Ma et al. [6] has published a review on applications of fault detection and diagnosis methods on NPPs. Effectiveness of fault-tolerant techniques in digital instruments was studied in [7]. Chao et al. [8] has combined deep neural networks with system performance models for hybrid deep fault detection and isolation. An improved Principal Component Analysis (PCA) method for detecting and isolating sensor faults in an NPP has been proposed in [9]. Mandal et al. [10] has proposed a statistical method for fault detection and isolation where an enhanced reconstruction method is presented using Enhanced Singular Value Decomposition (ESVD) for a Fast Breeder Test Reactor (FBTR).

ANN can solve nonlinear problems and hence it can be used effectively in fault detection and classification [11]. ANN is widely accepted, and it has the following features:

1) ANN can predict fast, reliably, and accurately depending on the training, because its working depends upon a series of very simple operations.

2) The nature of the nuclear reactor system changes with disturbances. Hence a neural network can incorporate the dynamic changes in the reactor systems.

Artificial Neural network (ANN) based fault detection technique for nuclear reactors has been proposed by Hwang et al. [11] and Elnokity et al. [12]. However, this technique deals mainly with sensor faults. In this paper, a fault detection technique of power sensors, coolant temperature sensors and actuators (control rod) has been established by

analyzing only two sensor data in a closed loop in presence of a robust PID controller. The fault detection problem becomes more challenging due to the robust PID controller, which can reject disturbances and has good tracking capability.

The remainder of the paper is organized as follows: Section II describes a Pressurized Water Reactor (PWR) type of NPPs. In Section III, details of ANN, data generation, training and detection technique are established. Section IV presents the credible MATLAB simulation for three cases: power sensor fault, coolant temperature sensor fault and actuator fault. Finally, Section IV concludes this work.

II. PWR WITH THERMAL HYDRAULIC MODEL

In this section, it is attempted to obtain an interval state-space model for a PWR [13]. A normalized point kinetic model of a PWR has been considered with a thermal-hydraulic model. The Xenon and Iodine dynamics are of less consequence during total power control, so they are not considered here.

The dynamic model is given by:

$$\frac{dP}{dt} = \frac{\rho_t - \beta}{\Lambda} P + \sum_{i=1}^{6} \lambda_i C_i \tag{1}$$

where $\beta = \sum_{i=1}^{6} \beta_i$

$$\frac{dC_i}{dt} = \beta_i \frac{P}{\Lambda} - \lambda_i C_i \tag{2}$$

where P is neutronic power, ρ_t is total reactivity, Λ is neutron generation time, λ_i , β_i , and C_i are decay constant, fraction of delayed neutrons, and delayed neutron precursors' concentration of i^{th} group, respectively.

The core thermal-hydraulics model is given by Mann's model [14] which considers two coolant lumps for every fuel lump,

$$\frac{dT_f}{dt} = H_f P - \frac{1}{\tau_f}\left(T_f - T_{c1}\right) \tag{3}$$

$$\frac{dT_{c1}}{dt} = \frac{1}{\tau_c}\left(T_f - T_{c1}\right) - \frac{2}{\tau_r}\left(T_{c1} - T_{cin}\right) \tag{4}$$

$$\frac{dT_{c2}}{dt} = \frac{1}{\tau_c}\left(T_f - T_{c1}\right) - \frac{2}{\tau_r}\left(T_{c2} - T_{c1}\right) \tag{5}$$

where T_f is average fuel temperature; T_{c1} and T_{c2} are average coolant temperatures in node 1 and node 2, respectively; T_{cin} is inlet temperatures of the first coolant node; H_f characterizes the rate of rise of fuel temperatures; τ_f and τ_c are time constants representing mean time for heat transfer from fuel to coolant and from core outlet to inlet, respectively while τ_r represents coolant residence time in the core. The heat transfer coefficient from fuel to coolant is assumed to be constant.

In this paper only the power control loop without secondary side coolant heat transfer has been considered. The change in total reactivity is considered due to the control rod movement and reactivity feedback due to fuel and coolant temperature. Here, a control rod acts as an actuator and this actuator movement can be represented by:

$$\frac{d\rho_{ex}}{dt} = Gz \tag{6}$$

where ρ_{ex} is the external reactivity injected to the reactor core due to the control rod movement, G is the reactivity worth of control rod while z is the speed of the control rod movement.

The total reactivity can be obtained by:

$$\rho_t = \rho_{ex} + \alpha_f T_f + \alpha_c T_{c1} + \alpha_c T_{c2} \tag{7}$$

where, α_f and α_c represent the temperature coefficients of reactivity due to fuel and coolant, respectively. Then (1)-(7) have been used to develop a nonlinear model of PWR. In this case itis assumed that, the input variable is controlling rod speed and the output variables are reactor power and coolant average temperature. In this paper, avoiding the detailed design of the sensor, sensor gain has been incorporated to the system, which is assumed to be linear for corresponding output. Next section will describe the procedure of the fault detection modeling.

III. FAULT DETECTION MODELLING

ANN has powerful non-linear mapping properties, noise tolerance, self-learning and parallel processing capabilities which add an important feature of a neural network used for prediction or estimation. It will also learn the dynamics of the system either to be linear or non-linear dynamic behavior during the learning session made over several learning cycles.

A. *Structure of ANN*

In this case, two networks are required as shown in table 1 and every network is built with two-layer feed-forward networks with sigmoid hidden neurons and linear output neurons. For the given consistent data and enough neurons in its hidden layer, this structure can fit multi-dimensional mapping problems.

Fig. 1 describes the structure of each NN. The number of neurons in the hidden layer for each network is different and it has been chosen by several runs of trial and error procedure and the best result has been taken for training. Table 1 shows the details of the network.

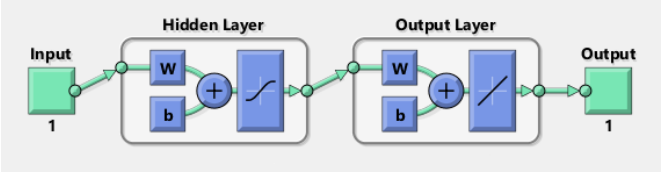

Figure 1. Structure of Neural Network (NN).

TABLE I. DIFFERENT NETWORK STRUCTURE

Network	Input	Hidden Layer	Output Layer	Output
NN1	Normalised demand power (X1)	5	1	Reactor Power (Y1)
NN2	Normalised demand power (X1)	6	1	Coolant Temperature (Y2)

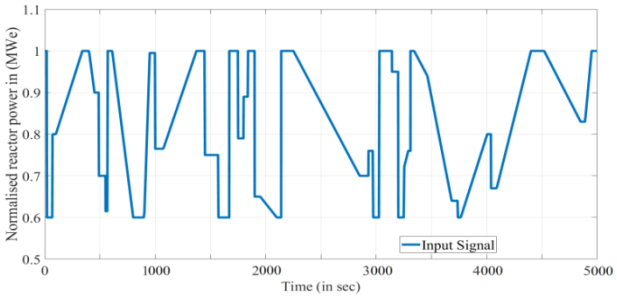

Figure 2. Random input signal.

B. *Data Generation and Training*

For ANN based fault detection, fault free input and output data are required for training purpose of ANN. The training data sets have been generated from the system simulation model described in section II, rather than actual operational plant data.

Fig. 2 depicts the random different combinations of demand power which is used as input data for the reactor system. Here, the power change has been considered within the range of 60% Full Power (FP)–100%FP for 5000 seconds with different pattern and magnitude between the above range as shown in Fig. 2. Next, the reactor model has been simulated without any fault with this random demand power described above. In this case, it has also been considered that a robust PID controller as described in [15] is working with the reactor model. The reactor output power (Y1) and the coolant temperature (Y2), corresponding to this input signal (X1), have been generated and stored in MATLAB workspace.

The networks are trained to adjust the weights to minimize the performance function. The gradient of the performance is determined using Levenberg–Marquardt (LM) backpropagation technique which involves performing computations backwards through the network. Mean Square Error (MSE) and Regression analysis (R) is used to test the performance. The average squared difference between outputs and targets is called MSE, lower values are better and zero means no error. The correlation between outputs and targets is measured by R values. R value= 1 means a close relationship while the same of 0 indicates a random relationship. The LM algorithm is the most used for adjustment of the parameters of the Multi-Layer Perceptron neural networks.

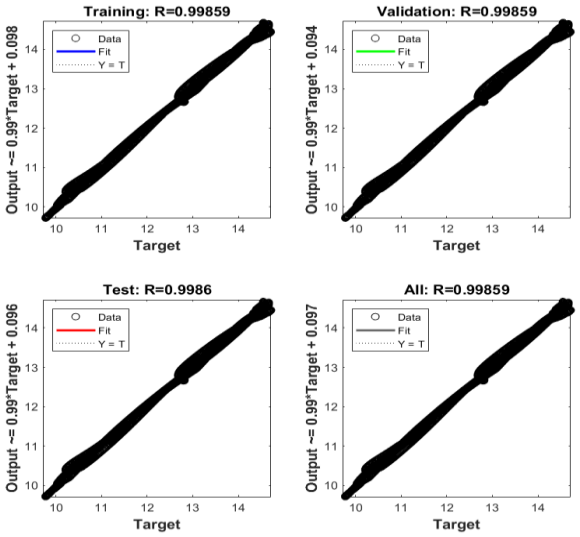

Figure 3. Regression analysis of NN1.

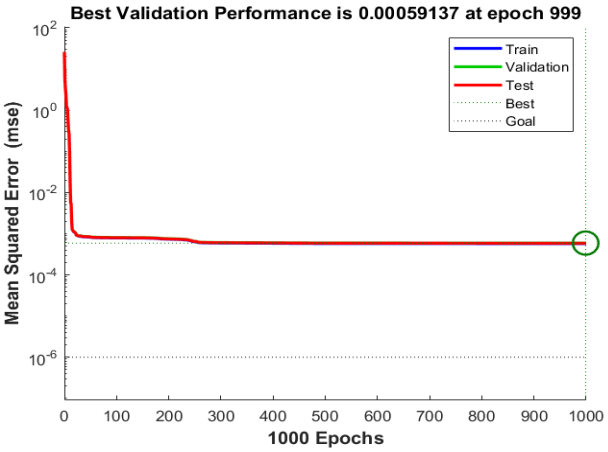

Figure 4. Performance analysis of NN1 using MSE.

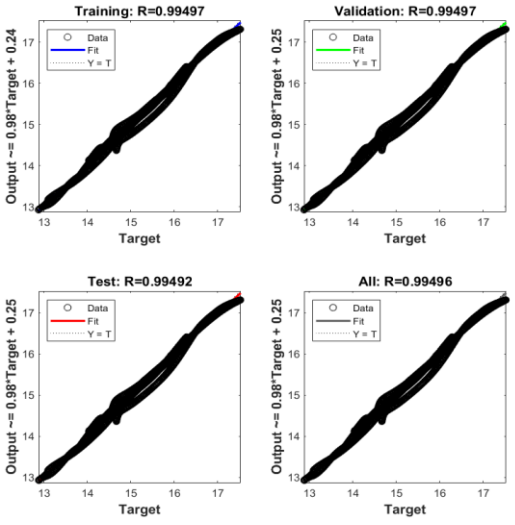

Figure 5. Regression analysis of NN2.

The training response curves of the two networks are shown in Fig. 3–Fig. 6. ANN training response for NN1 has been shown in Fig. 3 and Fig. 4 while Fig. 5 and Fig. 6 are for the NN2. Fig. 3 and Fig. 5 having four subplots represent the regression analysis during training at one epoch interval. Fig. 4 and Fig. 6 show the corresponding training performance. Those graphs depict that all networks have optimal successful results of training.

Actual power sensor output and NN1 output have been compared and generated a percentage error (e_1). Similarly, actual coolant sensor output has been compared with NN2 and generated a % error (e_2). The comparisons of NN1 and NN2 with the corresponding actual outputs are shown in Fig. 7 and Fig. 8 respectively.

C. Failure and Detection Technique

In this work, the sensor output of coolant temperature is not feedback to the reactor and only output from the power sensor is considered for the feedback. Thus, during a fault in the temperature sensor, there is no variation in e_1. Only e_2 will have a change in magnitude. But in case of power sensor failure, both e_1 and e_2 show a significant change. However, a PID controller in the closed loop will try to minimize e_1. As a result, in e_1 a sharp peak will appear while e_2 has a persistent value. In case of actuator saturation fault, the complete tracking is not possible so e_1 and e_2 both have a significant persistent value. e_1 and e_2 for all three faults have been shown in detail in Section IV in Figs. 12-13, Figs. 16-17 and Figs. 20-21 respectively. This technique has been depicted in Fig. 9 and used for fault detection.

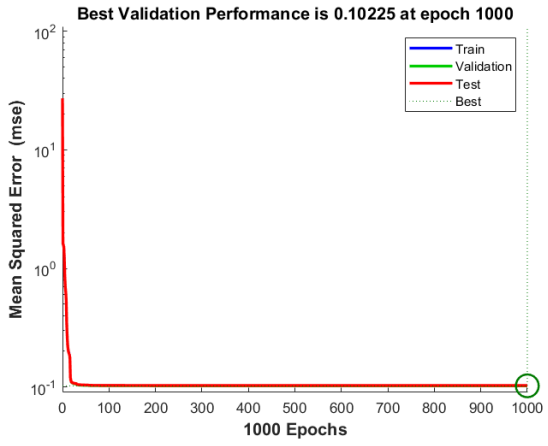

Figure 6. Performance analysis of NN2 using MSE.

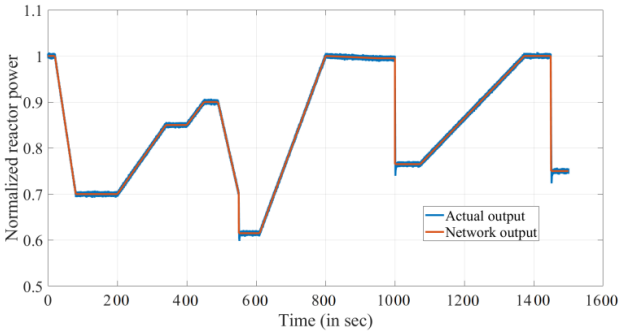

Figure 7. Network prediction with actual output with different data set of NN1.

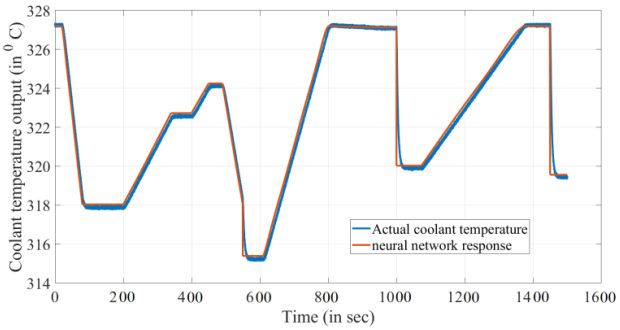

Figure 8. Network prediction with actual output with different data set of NN2.

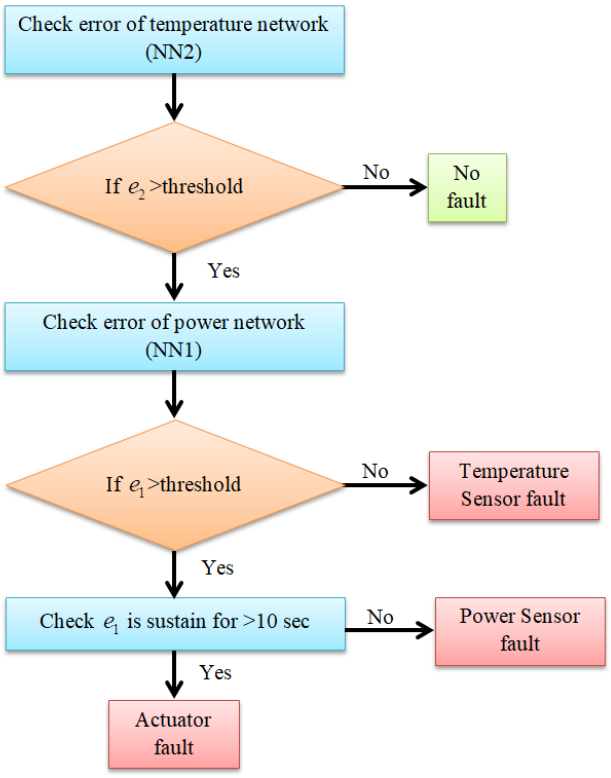

Figure 9. Flowchart for fault detection technique.

I. Simulation and Results

The trained ANNs based fault detection technique described in Section III is used to determine the faults in this section. In this paper, three fault cases have been carried out.

A. *Case1: Fault in Temperature Sensor*

First, it is assumed that the reactor is running at 100% FP. After 60 sec demand power is reduced to 80% FP at 10% FP/min ramp. The controller for the power loop is working well to handle this power maneuvering. Then at 200 sec, a random fault in temperature sensor bias within limit ±10% has been injected. Actual output power and coolant temperature have been shown in Figs. 10-11. Figs. 12-13 depict the error e_1 and e_2 respectively.

As only reactor power is acting as a feedback element, so during a fault in temperature sensor e_2 is not affecting the reactor power. So e_1 will remain in its tolerant limit, whereas e_2 has a persistent value as shown in Fig. 12 and Fig. 13. From Fig. 9 it can be referred to as a fault in temperature sensor.

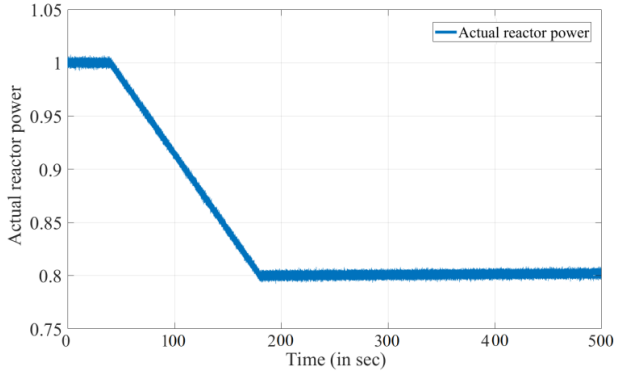

Figure 10. Actual normalized reactor power during fault in coolant temperature sensor.

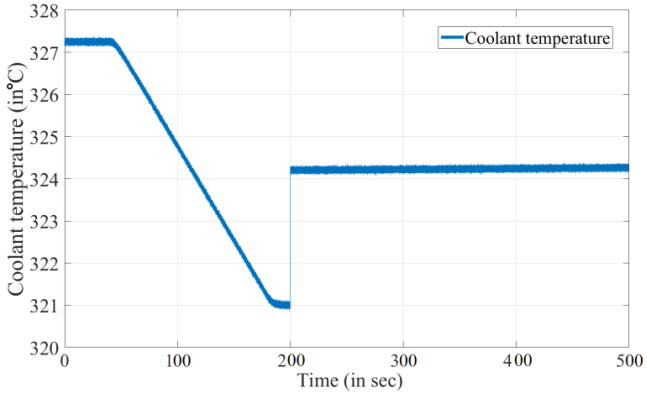

Figure 11. Actual coolant temperature during fault in coolant temperature sensor.

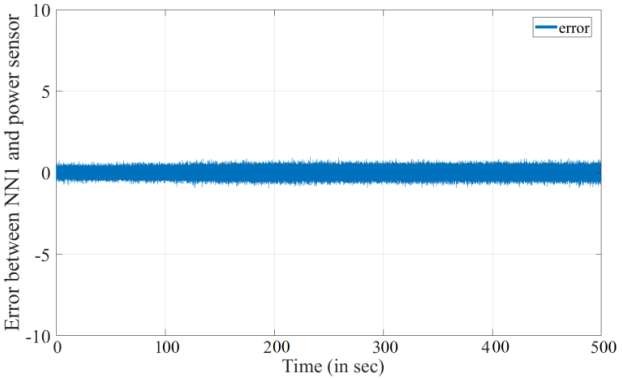

Figure 12. e_1 during fault in coolant temperature sensor.

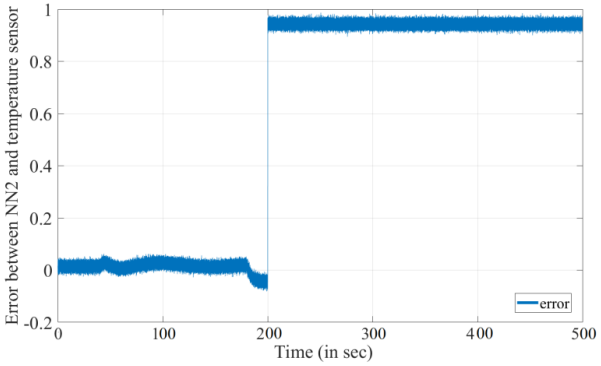

Figure 13. e_2 during fault in coolant temperature sensor.

B. *Case2: Fault in Power Sensor*

In this case, the initial condition of the reactor and the reduction of the demand power scenario has been considered and are same with earlier ones. At 210 sec, a random bias fault having limit ±5% has been injected. Corresponding actual reactor power, coolant temperature, e_1 and e_2 have been depicted in Fig. 14-Fig. 17 respectively.

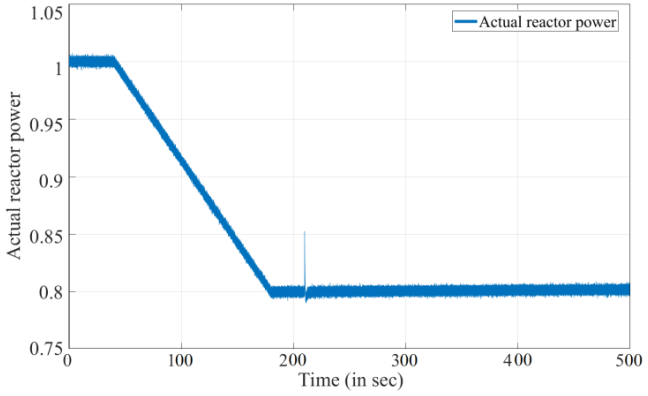

Figure 14. Actual normalised reactor power during fault in power sensor.

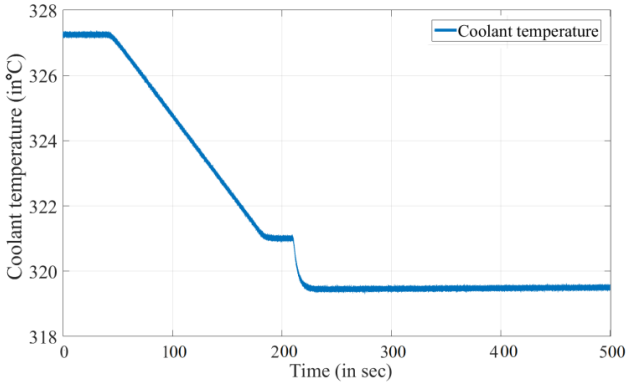

Figure 15. Actual coolant temperature during fault in power sensor.

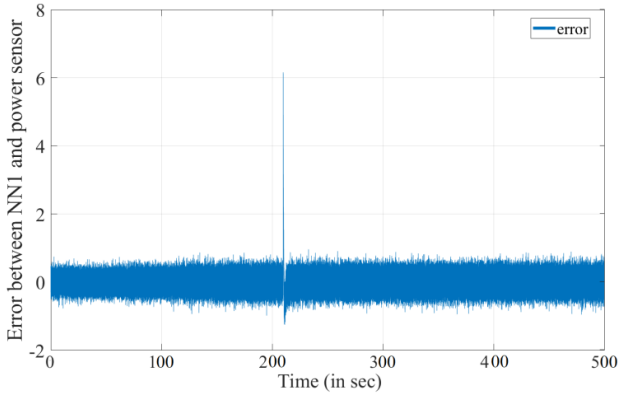

Figure 16. e_1 during fault in power sensor.

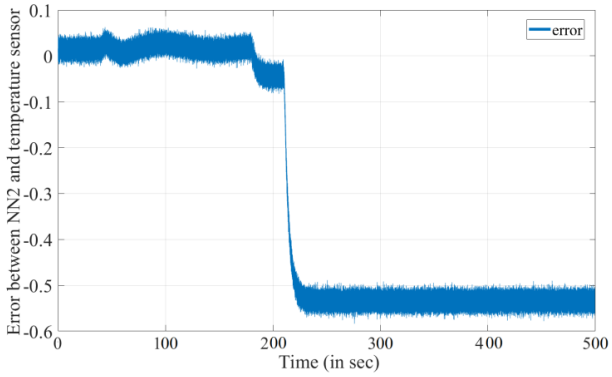

Figure 17. e_2 during fault in power sensor.

As described in the earlier section, the output from the power sensor is attached as a feedback connection. During a fault in the power sensor, the controller will try to track the reference signal which minimizes the process fault and e_1 as well. So, a peak will appear in e_1 as shown in Fig. 14. Again, this peak may appear as a prediction error during the transition period of fast ramping power maneuvering.

To avoid this confusion e_2 also is observed. If there is a fault in the power sensor, the controller will try to minimize the error by introducing more positive or negative reactivity depending upon the direction of the fault which will ultimately affect the coolant temperature. Thus, there always a non-zero steady deviation will appear in e_2 as depicted in Fig. 17. Owing to this situation it can be referred to as a fault in the power sensor.

C. Case3: Fault in Actuator (Control Rod)

In this case, again it assumed that the reactor is running at 100% FP and change in demand power are considered as earlier. During this transient, it is assumed that the control rod has been stuck in 90% of its actual position. Fig. 18-Fig. 21 depict the respective actual reactor power, coolant temperature, e_1 and e_2 respectively.

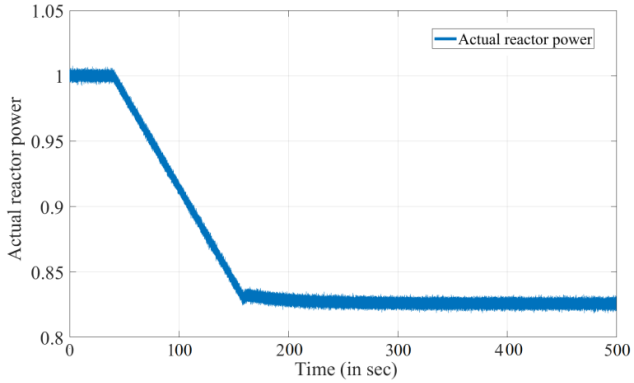

Figure18. Actual normalized reactor power during fault in actuator.

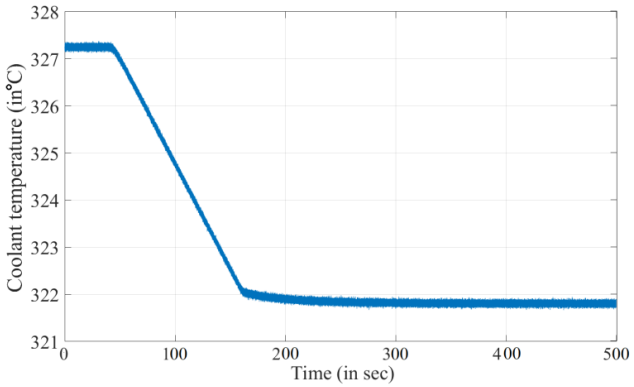

Figure 19. Actual coolant temperature during fault in actuator.

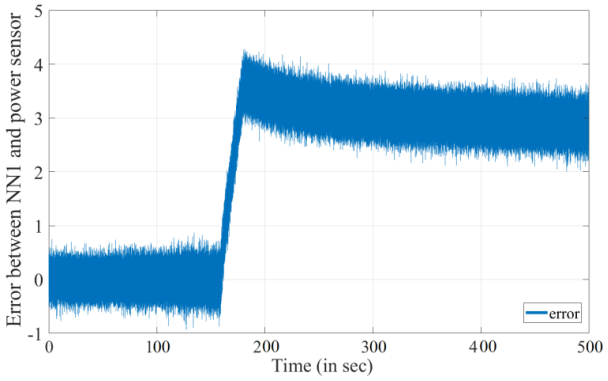

Figure 20. e_1 during fault in power actuator.

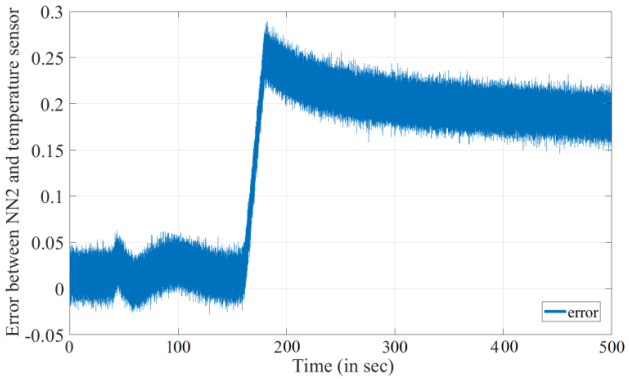

Figure 21. e_2 during fault in actuator.

In this case, the actual reactor power could not reach to 80%FP due to actuator saturation which will also affect the coolant temperature. Thus, in this case, e_1 and e_2 both will have a significant persistent value as shown in Fig. 20 and Fig. 21. which only happens due to actuator fault.

II. Conclusion

In this work, fault detection in sensors and actuators of a PWR type NPP has been established only using the power sensor data and coolant sensor data. Well performing ANNs have been created for power sensors and coolant sensors. Three faults and their detection technique have been shown with a credible simulation. However, this methodology is tested with a sensor bias fault only. As the sensor drift is a slow process it is a challenging task to apply this technique for detection of sensor drift. Further work can be carried out in that direction and isolation process.

Acknowledgment

The authors would like to thank Engineering and Physical Sciences Research Council (EPSRC) for their financial support with References: EP/R021961/1, EP/M018717/1, and EP/R022062/1.

References

[1] Upadhyaya, B.R., Zhao, K. and Lu, B., "Fault monitoring of nuclear power plant sensors and field devices," Progress in Nuclear Energy, 2003, 43(1-4), pp.337-342.

[2] Fernandes, R.G., Silva, D.R.C., de Oliveira, L.A.H.G. and Neto, A.D.D., "Faults detection and isolation based on neural networks applied to a levels control system," International Joint Conference on Neural Networks, 2007, August. (pp. 1859-1864). IEEE.

[3] Gautam, S., Tamboli, P.K., Roy, K., Patankar, V.H. and Duttagupta, S.P., "Sensors incipient fault detection and isolation of nuclear power plant using extended Kalman filter and Kullback–Leibler divergence," ISA transactions, 2019, 92, pp.180-190.

[4] Zhao, K. and Upadhyaya, B.R., "Adaptive fuzzy inference causal graph approach to fault detection and isolation of field devices in nuclear power plants," Progress in Nuclear Energy, 2005, 46(3-4), pp.226-240.

[5] Wang, H., Peng, M.J., Hines, J.W., Zheng, G.Y., Liu, Y.K. and Upadhyaya, B.R., "A hybrid fault diagnosis methodology with support vector machine and improved particle swarm optimization for nuclear power plants," ISA transactions, 2019, 95, pp.358-371.

[6] Ma, J. and Jiang, J., "Applications of fault detection and diagnosis methods in nuclear power plants: A review," Progress in nuclear energy, 2011, 53(3), pp.255-266.

[7] Kim, M.C., Seo, J., Jung, W., Choi, J.G., Kang, H.G. and Lee, S.J., "Evaluation of effectiveness of fault-tolerant techniques in a digital instrumentation and control system with a fault injection experiment," Nuclear Engineering and Technology, 2019, 51(3), pp.692-701.

[8] Arias Chao, M., Kulkarni, C., Goebel, K. and Fink, O., "Hybrid deep fault detection and isolation: Combining deep neural networks and system performance models," International Journal of Prognostics and Health Management, 2019, 10(033).

[9] Li, W., Peng, M. and Wang, Q., "Improved PCA method for sensor fault detection and isolation in a nuclear power plant," Nuclear Engineering and Technology, 2019, 51(1), pp.146-154.

[10] Mandal, S., Santhi, B., Sridhar, S., Vinolia, K. and Swaminathan, P., "Sensor fault detection in Nuclear Power Plant using statistical methods," Nuclear Engineering and Design, 2017, 324, pp.103-110.

[11] Hwang, B.C., Saif, M. and Jamshidi, M., "Neural based fault detection and identification for a nuclear reactor," IFAC Proceedings, 1993, Volumes, 26(2), pp.547-550.

[12] Elnokity, O., Mahmoud, I.I., Refai, M.K. and Farahat, H.M., "ANN based sensor faults detection, isolation, and reading estimates–SFDIRE: applied in a nuclear process," Annals of Nuclear Energy, 2012. 49, pp.131-142.

[13] Vajpayee, V., Becerra, V., Bausch, N., Deng, J., Shimjith, S.R., and Arul, A.J., "Dynamic modelling, simulation, and control design of a pressurized water-type nuclear power plant," Nuclear Engineering and Design, vol. 370, pp. 110901, 2020.

[14] Arda, S. E., and Holbert, K. E., "Nonlinear dynamic modeling and simulation of a passively cooled small modular reactor," Progress in Nuclear Energy, 2016, 91, pp. 116-131.

[15] Banerjee, S., Deng, J., Vajpayee, V., Becerra, V.M., Bausch, N., Shimjith, S.R. and Arul, J., "LMI based robust PID controller design for PWR with bounded uncertainty using interval approach," In 2019 7th International Conference on Control, Mechatronics and Automation (ICCMA) (pp. 253-259), IEEE.